

## MULTIPLE SERIES SOLUTIONS OF VISCOUS FLOWS OVER A STRETCHING/SHRINKING AND POROUS SHEET

by

**Azhar ALI<sup>a</sup>, Aziz KHAN<sup>b</sup>, Aftab ALAM<sup>c</sup>,  
Dil Nawaz Khan MARWAT<sup>c</sup>,  
Kamran<sup>c</sup>, and Thabet ABDELJAWAD<sup>b,d\*</sup>**

<sup>a</sup>Electrical Engineering Department, Sarhad University of Science and Information Technology, Peshawar, Pakistan

<sup>b</sup>Department of Mathematics and Sciences, Prince Sultan University, Riyadh, Saudi Arabia

<sup>c</sup>Department of Mathematics, Faculty of Technology and Engineering Sciences, Islamia College Peshawar, Pakistan

<sup>d</sup>Department of Medical Research, China Medical University, Taichung, Taiwan

Original scientific paper

<https://doi.org/10.2298/TSCI23S1185A>

*The viscous fluid-flow over a stretching (shrinking) and porous sheets of non-uniform thickness is investigated in this paper. The modeled problem is presented by utilizing the stretching/shrinking and porous velocities and variable thickness of the sheet. Consequently, the new problem reproduces the different available forms of flow motion maintained over a stretching/shrinking and porous sheet of variable thickness in one go. As a result, the governing equations are embedded in several parameters which can be transformed into classical cases of stretched/shrunk flows over porous sheets. A set of general, unusual and new variables is formed in order to simplify the governing PDE and boundary conditions. Three different series solutions of the final ODE are presented. A single analytical solution is not sufficient to predict the exact effects of all parameters on the flow field properties. The problem is solved by a power and two asymptotic series methods. The results are verified by providing a powerful numerical solution the problem. A complete set of solutions is provided and comparison of the solutions with classical models is established for appropriate values of the parameters which is shown in different graphs and tables.*

Key words: permeable (impermeable) and moving sheet, series solutions

### Introduction

Fluid-flows over stretching surfaces have numerous applications in engineering, physics and other field of sciences. The experimental investigations which exactly satisfy the theoretical studies of the physical phenomena can be found in [1]. The first paper appeared regarding fluid-flows due to stretching surfaces is presented by Sakiadis [2]. Later on this work is further verified and extended by Tsou *et al.* [3] and the theoretical results are closely matched with the experimental data. An exact solution of flows due to linear stretching is guaranteed by Crane [4] and further this model is equipped with mass suction (injection) at sheet surface [5]. The stretching problem is presented with certain generalizing factors and the modified approach can be found in [6]. Stretching (shrinking) problems are invariably

\* Corresponding author, e-mail: tabdeljawad@psu.edu.sa

attempted by reducing the governing strong non-linear boundary value problem into self-similar ODE and then solved exactly, analytically or numerically thereof. Many celebrated solutions have been found for the laminar boundary-layer flows past a stretching flat plate. However, the non-linear behavior of the modeled equations naturally deviates to the numerical solutions of the problem. The governing equations exhibit many characteristics of the thin sheet region or boundary-layer behavior. This is the reason many researchers evaluated the thickness of the boundary-layer and computed velocity profile of the flow problem. Since the boundary-layer thickness and velocity profiles play a significant role in the understanding of the behavior of such flows in industrial problems. Moreover, some properties have been investigated both numerically and analytically for such different problems [7-10]. In some cases the exact solutions of the modeled problem are provided. The power and asymptotic series solutions are the simplest and cheapest techniques, used for finding the solution of non-linear problems. Non-linear phenomena appeared in broad scientific fields like applied mathematics, and engineering. Scientists in those disciplines constantly face the task of finding solutions of non-linear ODE.

In this paper we introduced an interesting and mathematically compact, new and generalized similarity transformation for stream function and similarity variable and hence present a most modified form of transformations. These transformations are used to simplify the boundary value PDE and provide an exact boundary value ODE. Further, these transformations give rise to a new set of parameters which is playing its role in controlling the suction (injection), stretching (shrinking), and the thickness of the sheet (boundary deformation). Also, we concentrate on different solutions of the flow problem when a viscous and incompressible fluid past a porous and stretched (shrunk) sheet. We found different exact and series solutions of the non-linear problem. One analytical solution is not sufficient to describe all parameters values at one go. This is the reason, we attempt three different analytical series solutions. Accuracy of the series solution is insured such that all these series solutions are confirmed with the help of numerical method *i.e.* shooting method. An asymptotic solution is exactly converged to the closed form exact solution. Moreover, a power series solution when coupled with Pade approximation is attempted. These series solutions are very simple and straight forward without the needs of perturbation, linearization, discretization and rapidly infinite convergence.

### Similarity equations

Continuity and momentum equations subject to the kinematic boundary conditions at the surface of the sheet:

$$\frac{\partial u}{\partial x} + \frac{\partial v}{\partial y} = 0 \quad (1)$$

$$u \frac{\partial u}{\partial x} + v \frac{\partial v}{\partial y} = \nu \frac{\partial^2 u}{\partial y^2} \quad (2)$$

$$u(x, y) = U_w(x), v(x, y) = V_w(x) \text{ at } y = f(x) \quad (3)$$

$$u(x, y) = U_\infty(x) = 0 \quad (4)$$

The velocity field has two-components,  $u(x, y)$  and  $v(x, y)$  in  $x$ - and  $y$ -directions, respectively. Note that geometry of sheet is defined by a known function of  $x$  and variable stretching (shrinking) and porous velocities are taken.

Also note that

$$f(x) = A\sqrt{d_2}\alpha^\beta, \quad \alpha = d_0 + (d_1 + 2d_2)A_1x, \quad \text{and} \quad \beta = \frac{d_1 + d_2}{d_1 + 2d_2}$$

Also

$$U_w(x) = \frac{B}{d_2} A_2 \alpha^{1-2\beta} \quad \text{and} \quad V_w = \frac{c_1}{\sqrt{d_2}} A_1 A_2 \alpha^{-\beta}$$

are stretching (shrinking) and injection (suction) velocities, respectively. Further,  $V_w > 0$  ( $U_w > 0$ ) for injection (stretching),  $V_w < 0$  ( $U_w < 0$ ) for suction (shrinking) and  $V_w = 0$  ( $U_w = 0$ ) correspond to an impermeable (fixed) sheet. Further  $A, A_1, A_2, B, c_1, d_0, d_1,$  and  $d_2$  are the controlling parameters. The kinematic viscosity,  $\nu = \mu/\rho$ , coefficient of fluid viscosity,  $\mu$ , and density,  $\rho$ , are constants in the flow region.

Introducing the following similarity transformations in terms of stream function  $\psi$  and similarity variable  $\eta$ :

$$\psi = A_2 \frac{\alpha^{1-\beta}}{\sqrt{d_2}} f(\eta) \quad \text{and} \quad \eta = \frac{y}{\sqrt{d_2}} \alpha^{-\beta} \tag{5}$$

where  $\eta$  and  $f(\eta)$  are similarity variable and unknown function, respectively. The stream function is satisfying the relations  $u = \partial\psi/\partial y$  and  $v = \partial\psi/\partial x$ . In view of these definitions, eq. (1) is identically satisfied and by substituting the transformations defined in eq. (5) into eqs. (2)-(4), we obtained the exact boundary value ODE:

$$f''' + \delta_1 f'^2 + \delta_2 f f'' = 0 \tag{6}$$

$$f(A) = \delta_3, \quad f'(A) = B, \quad f'(\infty) = 0 \tag{7}$$

where

$$\delta_1 = \frac{A_1 A_2 d_1}{\nu}, \quad \delta_2 = \frac{A_1 A_2 d_2}{\nu}, \quad \text{and} \quad \delta_3 = \frac{-c_1 + AB(d_1 + d_2)}{d_2}$$

In the following sections we are emphasized on the asymptotic and power series solutions of the BVP given previously in eqs. (6) and (7). The solutions are accurate and confirmed by comparing it with the existing numerical and exact solutions.

### Series solutions

In this section, three different series solutions of the BVP (6) and (7) are presented.

#### Asymptotic series Solution I

An asymptotic series solution of the modeled problem is attempted and this type of series solutions are proposed in [11, 12] and for the solution of non-linear BVP. Asymptotic series solution of this special format is given:

$$f(\eta) = \sum_{n=0}^{\infty} a_n e^{-nc\eta}, \quad \text{for } c > 0 \tag{8}$$

All the coefficients,  $a_n$ , in the aforementioned series are need to be determined when the expression is substituted into ODE (6) and (7). Invoking the assumed solution in eq. (8) into BVP (6) and (7) yields:  $a_0 = c/\delta_2$  and the recurrence relation for  $a_n$ :

$$a_n = \sum_{i=1}^{n-1} \frac{[\delta_1 i(n-i) + \delta_2 (n-i)^2] a_i a_{n-i}}{cn^2(n-1)}, \quad n > 1$$

More coefficients  $a_n$  are calculated from the recurrence relation for  $2 \leq n \leq 4$ . All these coefficients are appeared in term of  $a_1$  and  $c$ :

$$a_2 = \frac{(\delta_1 + \delta_2) a_1^2}{4c}, \quad a_3 = \frac{(\delta_1 + \delta_2)(4\delta_1 + 5\delta_2) a_1^{33}}{27c^2}, \quad \text{and} \quad a_4 = \frac{(\delta_1 + \delta_2)(21\delta_1^2 + 53\delta_2 + 34\delta_2^2) a_1^4}{1728c^{33}}$$

The coefficients  $a_n$  are not noted here because of massive calculation and further terms are calculated with the help of MATHEMATICA. Obviously the series solution in eq. (8) is satisfying the infinity condition presented in BVP (6) and (7). The constant  $c$  and  $a_1$  are determined from eq. (8) when the boundary conditions of BVP (6) and (7) are used. Note that the solution in eq. (8) is only valid for  $\delta_1 + \delta_2 \neq 0$ . Moreover, when  $\delta_1 + \delta_2 = 0$ , the solution in eq. (8) is reduced to an exact solution. This exact solution has the closed form:

$$f(\eta) = \frac{c}{\delta_2} + a_1 e^{-c\eta}$$

In which

$$c = \frac{1}{2} \left( \delta_2^2 \pm \sqrt{\delta_2} \sqrt{4B + \delta_2^3} \right) \quad \text{and} \quad a_1 = \frac{\delta_2^{2/3} \pm \sqrt{4B + \delta_2^3}}{2\sqrt{\delta_2}}$$

### Asymptotic series Solution II

Consider the asymptotic series solution of ODE in BVP:

$$f(\eta) = \sum_{n=1}^{\infty} \frac{\alpha_n}{(\alpha + b\eta)^n} \quad (9)$$

where the coefficients  $\alpha_n$  are determined by substituting the aforementioned series (9) into BVP (6) and (7), and the recurrence relation is obtained for  $\alpha_n$ :

$$\alpha_n = \frac{\sum_{i=2}^{n-1} (n+1-i)(i\delta_1 + (n+2-i)\delta_2) \alpha_i \alpha_{n+1-i}}{n(n+1)(n+2)b - \alpha_1 [2k\delta_1 + (n(n+1) + 2)\delta_2]}, \quad \text{for } n \geq 3 \quad (10)$$

Note that

$$\alpha_1 = \frac{6b}{(\delta_1 + 2\delta_2)} \quad \text{and} \quad \delta_1 + 2\delta_2 \neq 0$$

More coefficients are calculated from the recurrence relation in eq. (10) and all these coefficients are appeared in term of  $\alpha_2$ ,  $\delta_1$ ,  $\delta_2$ , and  $b$  which are:

$$\alpha_3 = \frac{(\delta_1 + 2\delta_2)^2 \alpha_2^2}{6b}, \quad \alpha_4 = \frac{(\delta_1 + 2\delta_2)^2 \alpha_2^3}{6^2 b^2}, \quad \text{and} \quad \alpha_5 = \frac{(\delta_1 + 2\delta_2)^2 \alpha_2^3}{6^2 b^2}$$

These coefficients,  $\alpha_n$ , are generating a geometric sequence with the common ratio:

$$\frac{(\delta_1 + 2\delta_2)\alpha_2}{6b}$$

and its general term has the standard form:

$$\alpha_k = \frac{(\delta_1 + 2\delta_2)^{k-2} \alpha_2^{k-1}}{6^{k-2} b^{k-2}}, \quad i+2 \rightarrow k, \quad \text{for } i=1, 2, 3, \dots, n \quad (11)$$

Substituting the values of the coefficients from eq. (11) into eq. (9) we obtained:

$$f(\eta) = \frac{\alpha_1}{(a+b\eta)} + \frac{\alpha_2}{(a+b\eta)^2} + \sum_{n=3}^{\infty} \frac{(\delta_1 + 2\delta_2)^{n-2} \alpha_2^{n-1}}{6^{n-2} b^{n-2} (a+b\eta)^n} \quad (12)$$

The series in eq. (12) is an infinite geometric series with common ratio:

$$\left| \frac{(\delta_1 + 2\delta_2)\alpha_2}{6b(a+b\eta)} \right| < 1$$

and converges to

$$\frac{[6b(a+b\eta)]^2}{[6b(a+b\eta)]^2 - (\delta_1 + 2\delta_2)\alpha_2}$$

Finally the series solution in eq. (12) is reduced to the closed form solution:

$$f(\eta) = \frac{36b^2}{(\delta_1 + 2\delta_2)[6b(a+b\eta) - (\delta_1 + 2\delta_2)\alpha_2]} \quad (13)$$

The constants  $a$ ,  $b$ , and  $\alpha_2$  are determined by applying the conditions of BVP (6) and (7) which have the values:

$$a = \frac{\alpha_1}{\delta_3}, \quad b = -\frac{B\alpha_1}{\delta_3^2}, \quad \alpha_2 = 0, \quad \text{and } B = \frac{-\delta_1\delta_3^2 - 2\delta_2\delta_3^2}{6}$$

### Power series solution

Remember that the solution in eq. (13) is not working for  $\delta_1 + 2\delta_2 = 0$  where  $2\delta_2 \neq 0$ . Therefore, we are searching for a power series solution of BVP (6) and (7). Consider the power series solution of the problem:

$$f(\eta) = \sum_{n=0}^{\infty} \beta_n \eta^n \quad (14)$$

A recurrence relation for  $\beta_n$  is formed in the following equation when the series in eq. (14) is substituted into the condition of BVP (6) and (7). Since special values are assigned to the first two coefficients i.e.,  $\beta_0 = \delta_3$ ,  $\beta_1 = B$ , and  $\delta_1 + 2\delta_2 = 0$  with  $\delta_2 \neq 0$ :

$$\beta_{n+3} = \frac{\delta_2 \left[ 2 \sum_{i=1}^{n+1} i(n+2-i)\beta_i \beta_{n+2-i} - \sum_{i=0}^n (n+1-i)(n+2-i)\beta_i \beta_{n+2-i} \right]}{(n+1)(n+2)(n+3)}, \quad \text{for } n \geq 0 \quad (15)$$

Other coefficients  $\beta_n$  for fixed values of  $n$  are calculated from the aforementioned recurrence relation and all these coefficients are appeared in term of arbitrary constant  $\beta_2$  and parameters  $B$  and  $\delta_3$  which are:

$$\beta_3 = \frac{1}{3} \delta_2 (B^2 - \delta_3 \beta_2), \quad \beta_4 = \frac{1}{12} \delta_2 \left[ 3B\beta_2 + \delta_2 \delta_3 (-B^2 - \delta_3 \beta_2) \right] \text{ and}$$

$$\beta_5 = \frac{1}{60} \delta_2 \left[ 6\beta_2^2 - \delta_2^2 (B^2 + \delta_3 \beta_2) - \delta_2 (2B^3 - 5\delta_3 B \beta_2) \right]$$

Note that the recurrence relation in eq. (15) is obtained, with an arbitrary  $\beta_2$  which can be determine by using the infinity condition with the help of Pade approximation.

### Numerical solution

#### *Comparison of the series solutions with published and numerical results and graph discussion*

In this section, we present the numerical solution of the third order, non-linear ODE (6), satisfying the boundary condition (7). Also a comparative study of series solutions with classical results and numerical results is carried out to establish the accuracy of series solutions. Series solution in eq. (8) is the uniformly valid solution of BVP (6) and (7) for appropriate ranges of parameters values. All possible roots of arbitrary constants  $a_1$  and  $c$  are evaluated numerically with the help of MATHEMATICA. Accuracy of the series solution in eq. (8) is established by comparing it with the previous published results and numerical solution of the BVP (6) and (7). This task is simply achieved when different profiles of  $f'(\eta)$  are plotted in fig. 1 and compared with the exact solutions of [13] for the following three different cases. In addition that we have also compared the results of eq. (8) with the corresponding numerical solutions of the BVP (6) and (7) and the results are shown oin fig. 8(d).

*Case I:* When  $\delta_1 = \delta_2$ : The current result in eq. (8) is compared with literature and analyzed the behavior of  $\delta_1$  and  $\delta_2$  on velocity profiles for  $\delta_3 = 1$  and  $B = 1$ . The series solution in eq. (8) is exactly matched with the published results of eq. (12) in [13] and these profiles are plotted in fig. 1(a). It is noticed from this figure that the velocity profiles are decreased with increasing values of  $\delta_1$  when stretching is taken into account. The shapes of the profiles are changed smoothly with  $\delta_1$  and  $\delta_2$  over the range and no odd or unstable behavior has been seen. The parameter  $\delta_1$  tends to draw the profiles towards the wall as shown in fig. 1(a).

*Case II:* When  $\delta_1 \neq \delta_2$ : The condition (*i.e.*  $\delta_1 \neq \delta_2$ ) is analogous with the exact solution of eq. (15) in [13], therefore, the asymptotic series solution in eq. (8) is compared with it and excellent agreement between the two is found. For fixed value of  $\delta_1 = -1$  and shrinking parameter  $B = -1$ , effects of  $\delta_2$  and  $\delta_3$  on velocity profiles is shown in fig. 1(b). With the boosting values of  $\delta_2$  and declining values of  $\delta_3$  velocity profiles are decreased.

*Case III:* When  $\delta_1 = -\delta_2$  ( $\delta_2 > 0$ ): In this case we have chosen different values for suction and stretching parameters *i.e.*  $\delta_3 = -1$  and  $B = 1$  in order to compare the results of eq. (8) with exact solution in eq. (18) of [13]. All these profiles have been plotted in fig. 1(c). The two results are exactly matched and fluid velocity is decreased with the increasing values of  $\delta_2$ .

*Case IV:* Comparison with numerical solution: The series solution in eq. (8) is also compared with the numerical solution of BVP (6) and (7) and plotted in fig. 1(d). In this part of fig. 1,  $f'$  is plotted against  $\eta$  and computed from two different solutions. The numerical results are obtained by Shooting method, and effects of suction (injection) parameter is seen

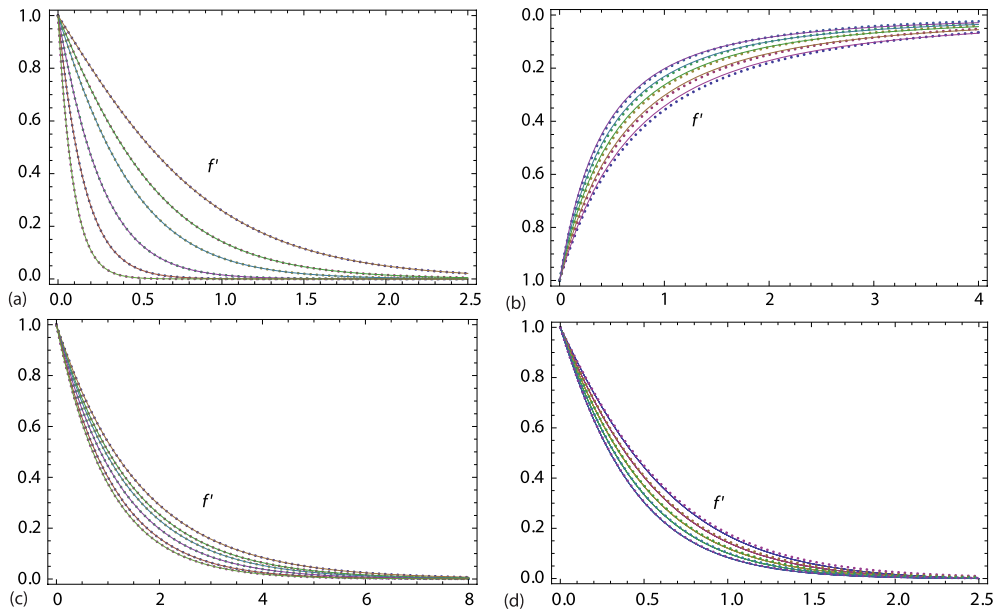


**Figure 1.** (a) The  $f'$  is plotted against  $\eta$  from eq. (8) for  $\delta_2 = \delta_1 = 1$  (top profile), 1.5, 2, 3.5, 6, and 10.5 (bottom profile), present solution (.....) and solution of eq. (12) form [13] (\_\_\_\_) where  $\delta_3 = B = 1$ , (b) the  $f'$  is plotted against  $\eta$  from eq. (8) for  $\delta_1 \neq \delta_2$  and  $(\delta_2, \delta_3) = (2, 2^{1/2})$  (bottom profile), (2.5, 1.22474), (3.2, 1.05409), [4,  $(6/7)^{1/2}$ ], [5,  $(2/3)^{1/2}$ ] (top profile), present solution (.....) and solution of eq. (15) form [13] (\_\_\_\_) where  $\delta_1 = B = -1$ , (c) the  $f'$  is plotted against  $\eta$  from eq. (8) for  $\delta_1 = \delta_2$  ( $\delta_2 > 0$ ) = 1 (top profile), 1.5, 2, 3.5, 6, 10, and 60. 5 (bottom profile), present solution (.....) and solution of eq. (18) form [13] (\_\_\_\_) where  $\delta_3 = -1, B = -1$ , and (d) the  $f'$  is plotted against  $\eta$  from eq. (8) for different  $\delta_3 = 1.4$  (top profile), 1.6, 1.8, 2.0, and 2.2 (bottom profile), analytic solution (.....) and numerical solution (\_\_\_\_) where  $\delta_1 = \delta_2 = B = 1$

on fluid-flow for fixed values of  $B, \delta_1$  and  $\delta_2$ . The velocity profiles are analyzed for increasing values of injection parameter  $\delta_3$  in fig. 1(d). With the increasing values of  $\delta_3$ , velocity of the fluid is decreased. For this case the numerical and analytical solutions are exactly matched with each other. At the vicinity of sheet, differences between numerical and analytical results are bit higher for  $\delta_3 = 1.4$ , and acceptable results have been obtained. Moreover, the series solution in eq. (8) is also compared for  $f''(\eta)$  with the numerical results for which different values are assigned to parameters and the results are shown in tab. 1. In this table, the numerical solution of BVP (6) and (7) and analytical results in eq. (8) are compared and the two results are also compared with the published data of [12, 14-16]. Note that different values of the missing constants  $c$  and  $a_1$  are taken and evaluated from eq. (8) with MATHEMATICA when conditions of BVP (6) and (7) are used. Strong resemblance is found among these results and shown in tab. 1. The second asymptotic series solution in eq. (13) is compared with the numerical and exact solutions and the results are exactly matched to each other when different values are given to  $\delta_2, \delta_3$ , and  $B > 0$ . The results are plotted in fig. 2(a). It is observed that the velocity is decreased with the increasing of  $\delta_2$  and decreasing of  $\delta_3$  for fixed values of  $\delta_1 = -1$  and  $\alpha_2 = 0$ . Since the BVP (6) and (7) has semi-infinite domain and its power series solution has been attempted, the solution in eq. (14) is carried out with the infinity condition of BVP (6) and (7), using the diagonal Padé approximation of order  $[N/N] = [5/5]$ . One can see the detail of diagonal Pade

approximation in [17]. In order to claim the validity and accuracy of power series solution, we compared  $f'(\eta)$  from eq. (8) for fixed values of  $\delta_1$ ,  $\delta_2$ , and  $\delta_3$  with the numerical solution and absolute error between solutions is shown in tab. 2 and different profiles of  $f'(\eta)$  are plotted in fig. 2(b) using the diagonal Pade approximation  $[N/N] = [5/5]$ . In fig. 2(b), we noticed that velocity profiles is decreased with decreasing values of  $\delta_2$  for fixed values of suction and shrinking parameters  $\delta_3 = -1, B = -1$ .

**Table 1. The  $f''(0)$  is computed numerically and analytically from the BVP (6) and (7), and eq. (8), respectively**

$\delta_3$	$c$	$a_1$	$\delta_1$	$\delta_2$	Numeric	Analytic	Previous results
0	0.783599	-1.94083	-0.1	0.5	-0.5045	-0.504472	-0.5044714296 [14]
0	0.707107	-1.41421	-0.5	0.5	-0.7071	-0.707107	-0.7071067812 [14]
0	0.640387	1.03778	-1.0	0.5	-0.9064	-0.906376	-0.9063755237 [14]
0	1	-1	-1.0	1.0	-1.0	-1.0	-1.0 [12, 16, 18]
-1	0.388468	-1.17906	-1.0	0.5	-0.7085	-0.70853	-0.708761 [15]
1	0.965555	-0.834067	-1.0	0.5	-1.1756	-1.17561	-1.17561409 [15]

**Table 2. The  $f'(\eta)$  is computed numerically and analytically from BVP (6) and (7) and eq. (14) for  $B = 1, \delta_3 = -1/5$**

$\eta$	$\delta_2 = -1/6$			$\delta_2 = -4/21$			$\delta_2 = -5/36$		
	Numeric	analytic	abs. error	Numeric	analytic	abs. error	Numeric	analytic	abs. error
0	-1	-1	0.0	-1	-1	0.0	-1	-1	0.0
0.4592	-0.7964	-0.78536	$1.10 \cdot 10^{-2}$	-0.7848	-0.77224	$1.26 \cdot 10^{-2}$	-0.8116	-0.8022	$9.40 \cdot 10^{-3}$
1.8367	-0.4251	-0.40232	$2.28 \cdot 10^{-2}$	-0.4033	-0.37856	$2.47 \cdot 10^{-2}$	-0.4546	-0.43449	$2.01 \cdot 10^{-2}$
2.7551	-0.2888	-0.26588	$2.29 \cdot 10^{-2}$	-0.2681	-0.24356	$2.45 \cdot 10^{-2}$	-0.3176	-0.29699	$2.06 \cdot 10^{-2}$
3.5204	-0.212	-0.19061	$2.14 \cdot 10^{-2}$	-0.1935	-0.17077	$2.27 \cdot 10^{-2}$	-0.2383	-0.21885	$1.95 \cdot 10^{-2}$
4.5918	-0.1349	-0.12106	$1.83 \cdot 10^{-2}$	-0.1243	-0.10503	$1.93 \cdot 10^{-2}$	-0.1613	-0.14453	$1.68 \cdot 10^{-2}$
5.5102	-0.098	-0.08257	$1.54 \cdot 10^{-2}$	-0.0858	-0.06953	$1.63 \cdot 10^{-2}$	-0.1163	-0.10209	$1.42 \cdot 10^{-2}$
6.5816	-0.0652	-0.05296	$1.22 \cdot 10^{-2}$	-0.0559	-0.04286	$1.30 \cdot 10^{-2}$	-0.0795	-0.06845	$1.10 \cdot 10^{-2}$
7.6531	-0.0433	-0.0339	$9.40 \cdot 10^{-3}$	-0.0363	-0.02614	$1.02 \cdot 10^{-2}$	-0.0543	-0.04606	$8.24 \cdot 10^{-3}$
8.5714	-0.0303	-0.023	$7.30 \cdot 10^{-3}$	-0.025	-0.01684	$8.16 \cdot 10^{-3}$	-0.0389	-0.03285	$6.05 \cdot 10^{-3}$
9.4898	-0.021	-0.01549	$5.51 \cdot 10^{-3}$	-0.017	-0.0106	$6.40 \cdot 10^{-3}$	-0.0275	-0.02344	$4.06 \cdot 10^{-3}$
10	-0.017	-0.01239	$4.61 \cdot 10^{-3}$	-0.0136	-0.00808	$5.52 \cdot 10^{-3}$	-0.0225	-0.01944	$3.06 \cdot 10^{-3}$
10.5102	-0.0136	-0.00987	$3.73 \cdot 10^{-3}$	-0.0108	-0.00608	$4.72 \cdot 10^{-3}$	-0.0183	-0.01614	$2.16 \cdot 10^{-3}$
11.5306	-0.0085	-0.00622	$2.28 \cdot 10^{-3}$	-0.0116	-0.00327	$3.33 \cdot 10^{-3}$	-0.0116	-0.01116	$4.44 \cdot 10^{-4}$
12.6531	-0.0046	-0.00371	$8.93 \cdot 10^{-4}$	-0.0035	-0.00146	$2.04 \cdot 10^{-3}$	-0.0064	-0.00753	$1.13 \cdot 10^{-3}$
13.4649	-0.0026	-0.00257	$3.23 \cdot 10^{-5}$	-0.0019	-0.00071	$1.19 \cdot 10^{-3}$	-0.0036	-0.00575	$2.15 \cdot 10^{-3}$
14.4898	-0.0007	-0.0017	$1.00 \cdot 10^{-3}$	-0.0005	-0.00022	$2.80 \cdot 10^{-4}$	-0.001	-0.00425	$3.25 \cdot 10^{-3}$
15	0.0000	-0.00144	$1.44 \cdot 10^{-3}$	0.0000	-0.00011	$1.12 \cdot 10^{-4}$	0.0000	-0.00373	$3.73 \cdot 10^{-3}$



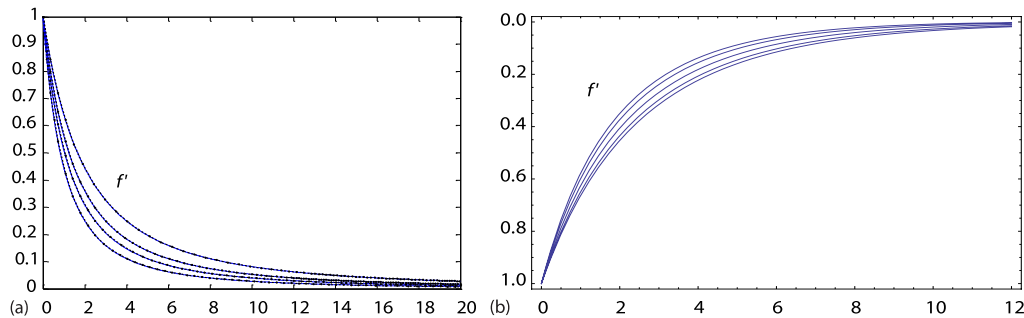


Figure 2. (a) The  $f'$  is plotted against  $\eta$  from eq. (13)  $(\delta_1, \delta_2) = (-0.25, -2)$  for (bottom profile),  $(0.02, -2.5)$ ,  $(1/6, -3)$ ,  $(5/16, -4)$  (top profile), where  $\delta_1 = -1$ ,  $B = 1$  and analytical and numerical solutions are represented by solid and dashed lines, respectively and (b) the  $f'$  is plotted against  $\eta$  from eq. (14) for  $\delta_2 = 1$  (top profile),  $-1/6$ ,  $-4/21$ ,  $-5/36$ ,  $-6/51$ , and  $-7/66$  (bottom profile) where  $\delta_3 = -1/5$ ,  $B = -1$

## Conclusion

The present model demonstrates flow over a vertical porous (both suction and injection can take place) and stretching (shrinking) sheet of variable thickness. The boundary-layer equations and boundary conditions are transformed into non-linear ODE by *introducing unusual and generalized similarity transformations* for the stream function and similarity variable. Three different series solutions of the modeled BVP (6) and (7) are presented here. All the series solutions are compared with numerical solution of the governing Navier-Stokes equations for an incompressible viscous fluid-flows over a stretching (shrinking) and permeable surfaces. Comparison between solutions is established in different tables and graphs and excellent agreement is found. Note that two exact solutions are retrieved from the series solutions for some conditions on the parameters values. Meanwhile, the series solution in eq. (8) is reduced to an exact solution for  $\delta_1 + \delta_2 = 0$  and  $\delta_2 \neq 0$ . The series solution in eq. (9) is converged to exact solution when  $\delta_1 + \delta_2 \neq 0$ . Two series solutions are exactly reduced to the existing exact solutions of [17] for special values of the parameters. All these results are shown in different graphs and tables. The series solutions are not working simultaneously for all choice of parameters value. Each series solution is compared with the numerical solution and excellent agreement is found.

## Acknowledgment

The authors Aziz Khan and T. Abdeljawad would like to thank Prince Sultan University for the support through the TAS research lab.

Funding: The authors Aziz Khan and T. Abdeljawad would like to thank Prince Sultan University for paying the APC of this article.

## References

- [1] Fisher, E. G., *Extrusion of Plastics*, Wiley, New York, USA, 1976
- [2] Sakiadis, B. C., Boundary-Layer Behavior on Continuous Solid Surface: II. Boundary-Layer on a Continuous Flat Surface, *Journal AIChE*, 7 (1961), 2, pp. 221-225
- [3] Tsou, F. K., et al., Flow and Heat Transfer in the Boundary-Layer on a Continuous Moving Surface, *International Journal of Heat Mass Transfer*, 10 (1967), 2, pp. 219-235
- [4] Crane, L. J., Flow Past a Stretching Plate, *Zeitschrift für angewandte Mathematik und Physik ZAMP*, 21 (1970), July, pp. 645-647
- [5] Gupta, P. S., Gupta, A. S., Heat and Mass Transfer on a Stretching Sheet with Suction or Blowing, *The Canadian Journal of Chemical Engineering*, 55 (1977), 6, pp. 744-746

- [6] Kuiken, H. K., On Boundary-Layers in Fluid Mechanics that Decay Algebraically along Stretches of Wall that Are not Vanishingly Small, *IMA Journal of Applied Mathematics*, 27 (1981), 4, pp. 387-405
- [7] Kechil, S., et al., Approximate Analytical Solutions for a Class of Laminar Boundary-Layer Equations, *Chinese Physics Letter*, 24 (2007), 1981
- [8] Shit, G. C., Haldar, R., Effects of Thermal Radiation on MHD Viscous Fluid-Flow and Heat Transfer over Non-Linear Shrinking Porous Sheet, *Applied Mathematics and Mechanics*, 32 (2011), June, pp. 677-688
- [9] Akbar, N., et al., Dual Solutions in MHD Stagnation-Point Flow of Prandtl Fluid Impinging on Shrinking Sheet, *Applied Mathematics and Mechanics*, 35 (2014), May, pp. 35813-35820
- [10] Zhu, Y., Experimental and Numerical Study of Flow Structures of the Second-Mode Instability, *Applied Mathematics and Mechanics*, 40 (2019), Jan., pp. 273-282
- [11] Cochran, W. G., The Flow Due to a Rotating Disc, *Mathematical Proceedings of the Cambridge Philosophical Society*, 30 (1934), 3, pp. 65-75
- [12] Ackroyd J. A. D. On the steady flow produced by a rotating disc with either surface suction or injection. *Journal of Engineering Mathematics*, 12 (1978), July, pp. 207-220
- [13] Azhar A., et al., New Approach to the Exact Solution of Viscous Flow Due to Stretching (Shrinking) and Porous Sheet, *Results in Physics*, 7 (2017), Mar., pp. 1122-1127
- [14] Liao, S. J., A New Branch of Solutions of Boundary-Layer Flows over an Impermeable Stretched Plate, *International Journal of Heat and Mass Transfer*, 48 (2005), 12, pp. 2529-2539
- [15] Liao, S. J., A New Branch of Solution of Boundary-Layer Flows over a Permeable Stretching Plate, *International Journal of Non-Linear Mechanics*, 42 (2007), 6, pp. 819-830
- [16] Wang, C. Y., Analysis of Viscous Flow Due to a Stretching Sheet with Surface Slip and Suction, Non-Linear Analysis: *Real World Applications*, 10 (2009), 1, pp. 375-380
- [17] Boyd, J. P., Pade Approximant Algorithm for Solving Non-Linear Ordinary Differential Equation Boundary Value Problems on an Unbounded Domain, *Computers in Physics*, 11 (1997), 3, pp. 299-303
- [18] Zaimi, K., Ishak, A., Boundary-Layer Flow and Heat Transfer over a Permeable Stretching/Shrinking Sheet with a Convective Boundary Condition, *Journal of Applied Fluid Mechanics*, 8 (2015), 3, pp. 499-505